

See discussions, stats, and author profiles for this publication at: <https://www.researchgate.net/publication/5902534>

CUL7 Is a Novel Antiapoptotic Oncogene

Article in *Cancer Research* · November 2007

DOI: 10.1158/0008-5472.CAN-07-0644 · Source: PubMed

CITATIONS

34

READS

28

13 authors, including:



[Lilia Kaustov](#)

University of Toronto

25 PUBLICATIONS 557 CITATIONS

[SEE PROFILE](#)



[Yi Sheng](#)

York University

44 PUBLICATIONS 828 CITATIONS

[SEE PROFILE](#)

Cancer Research

CUL7 Is a Novel Antiapoptotic Oncogene

Sam S. Kim, Mary Shago, Lilia Kaustov, et al.

Cancer Res 2007;67:9616-9622.

Updated version	Access the most recent version of this article at: http://cancerres.aacrjournals.org/content/67/20/9616
Supplementary Material	Access the most recent supplemental material at: http://cancerres.aacrjournals.org/content/suppl/2007/10/05/67.20.9616.DC1.html

Cited Articles	This article cites by 30 articles, 18 of which you can access for free at: http://cancerres.aacrjournals.org/content/67/20/9616.full.html#ref-list-1
Citing articles	This article has been cited by 7 HighWire-hosted articles. Access the articles at: http://cancerres.aacrjournals.org/content/67/20/9616.full.html#related-urls

E-mail alerts	Sign up to receive free email-alerts related to this article or journal.
Reprints and Subscriptions	To order reprints of this article or to subscribe to the journal, contact the AACR Publications Department at pubs@aacr.org .
Permissions	To request permission to re-use all or part of this article, contact the AACR Publications Department at permissions@aacr.org .

CUL7 Is a Novel Antiapoptotic Oncogene

Sam S. Kim,^{1,4} Mary Shago,¹ Lilia Kaustov,¹ Paul C. Boutros,^{1,2,4} James W. Clendening,^{1,4} Yi Sheng,¹ Grace A. Trentin,¹ Dalia Barsyte-Lovejoy,¹ Daniel Y.L. Mao,¹ Robert Kay,⁵ Igor Jurisica,^{2,3,4} Cheryl H. Arrowsmith,^{1,4} and Linda Z. Penn^{1,4}

Divisions of ¹Cancer Genomics and Proteomics and ²Signaling Biology, Ontario Cancer Institute and Departments of ³Computer Science and ⁴Medical Biophysics, University of Toronto, Toronto, Ontario, Canada and ⁵Terry Fox Laboratory, BC Cancer Research Centre, Vancouver, British Columbia, Canada

Abstract

Using an expression cloning approach, we identify CUL7, a member of the cullin family, as a functional inhibitor of Myc-induced apoptosis. Deregulated expression of the Myc oncogene drives cellular proliferation yet also sensitizes cells to undergo p53-dependent and p53-independent apoptosis. Here, we report that CUL7 exerts its antiapoptotic function through p53. CUL7 binds directly to p53, and small interfering RNA-mediated knockdown of CUL7 results in the elevation of p53 protein levels. This antiapoptotic role of CUL7 enables this novel oncogene to cooperate with Myc to drive transformation. Deregulated ectopic expression of c-Myc and CUL7 promotes Rat1a cell growth in soft agar, and knockdown of CUL7 significantly blocks human neuroblastoma SHEP cell growth in an anchorage-independent manner. Furthermore, using public microarray data sets, we show that CUL7 mRNA is significantly overexpressed in non-small cell lung carcinoma and is associated with poor patient prognosis. We provide experimental evidence to show CUL7 is a new oncogene that cooperates with Myc in transformation by blocking Myc-induced apoptosis in a p53-dependent manner. [Cancer Res 2007;67(20):9616–22]

Introduction

The members of the *myc* oncogene family, whose products play a major role in the etiology of human cancers, include c-Myc (*MYC*), N-myc (*MYCN*), and L-myc (*MYCL1*; ref. 1). All three oncoproteins function as regulators of gene transcription to orchestrate a wide variety of biological activities, including cell proliferation and apoptosis (1). Myc potentiation of apoptosis serves as an intrinsic safety mechanism to eliminate precancerous cells harboring this potent oncoprotein (2). Thus, genetic alterations that functionally block Myc-induced apoptosis dangerously unleash Myc to fully drive cellular proliferation and malignant transformation.

Myc can potentiate apoptosis by activating p53 and evidence shows that abrogation of the p53 pathway is a key event in tumorigenesis (3). In many tumors harboring deregulated Myc, however, cells are surprisingly resistant to apoptosis even without p53 mutations (4). These findings suggest that there must be oncogenes that

can inhibit p53 and cooperate with Myc to promote transformation. Here, we report CUL7 as a novel oncogene that cooperates with Myc to promote transformation.

Materials and Methods

Cell culture. The U2OS, Rat1MycERtm-myc, Rat1a, T47D, Phoenix Ampho, and Phoenix Eco cells (American Type Culture Collection) were maintained in 10% fetal bovine serum (FBS) DMEM H21. SHEP Tet21/N-Myc cells were maintained in 10% FBS RPMI 1640. All media were supplemented with 100 µg/mL penicillin and 100 µg/mL streptomycin sulfate.

Constructs. The plasmid pSK-KIAA0076 was obtained from the Kazusa DNA Research Institute (Chiba, Japan). The KIAA0076 insert (CUL7) was cloned into pBabeMNiresGFP retroviral vector at *EcoRI/XhoI* and into pBabepuro at *EcoRI/SalI*. pBabeMNiresGFP and pBabepuro retroviral constructs were modified by ligation of a FLAG tag at the NH₂ terminus of CUL7. pBabeMNiresGFP-Hu-cMyc was described previously (5). To generate MSCV-YFP-p53DD, p53DD insert was first obtained by digesting pSPp53DD (kind gift of Dr. Moshe Oren, Weizman Institute of Science, Rehovot, Israel) at *BamHI/SmaI* site and then cloned into *BglIII/HpeI* sites of pMSCV-YFP.

Retroviral production and infection. Infectious replication-deficient ecotropic retroviral particles were produced in Phoenix Eco cells and used to infect Rat1, Rat1a, and SHEP N-Myc cells expressing ecotropic receptor (5).

Functional screen. Rat1MycERtm-myc cells were either mock infected or infected with a retroviral library of cDNA from the T47D breast carcinoma cell line in the retroviral vector pCTV1 (6). Apoptotic conditions were maintained by changing the medium to 0.06% FBS and adding 0.1 µmol/L hydroxytamoxifen to activate MycERtm. The surviving cells were then replated and subjected to a second round of Myc-induced apoptosis. Subsequently, surviving colonies were picked and the retrovirally transduced cDNA was isolated from these cells by PCR of genomic DNA using primers specific for the provirus as described (6).

Immunoblot analysis. α-CUL7 antibodies were raised against a synthetic COOH-terminal peptide RGVYPASCTATQSFSTFR (human CUL7 amino acids 1,681–1,698) in rabbits. Immunoblots were probed with the COOH-terminal-specific CUL7 antibody or p53 antibody (DO-1; Santa Cruz Biotechnology). p53DD was immunoblotted with p53 antibody (Pab421) and c-Myc was probed with 9E10 antibody. Bcl2 was probed with polyclonal anti-Bcl2 antibody (kind gift of Dr. David Andrews, Department of Biochemistry, McMaster University, Hamilton, Ontario, Canada).

Cell death assay. Rat1MycERtm-myc (10⁶) cells were seeded in duplicate. After 24 h, medium was changed to 0.06% FBS and 0.1 µmol/L hydroxytamoxifen. Cells were harvested at 72 h, stained with propidium iodide, and analyzed by flow cytometry. For the CUL7 RNA interference (RNAi) experiments, SHEP Tet21/N-Myc MSCV-YFP and SHEP Tet21/N-Myc MSCV-YFP-p53DD cells were first infected with lentivirus expressing one of pLKO-Puro-luciferase small interfering RNA (siRNA), pLKO-Puro-CUL7 siRNA #2, or pLKO-Puro-CUL7 siRNA #5. One day after infection, the cells were selected with puromycin at 1 µg/mL concentration for 2 days. Cells were then seeded in triplicate on tissue culture plates, and 3 days after the seeding, both floating and adherent cells in triplicate tissue culture plates were harvested and analyzed by propidium iodide staining and flow cytometry. Cell death (% pre-G₁) was assessed by measurement of subdiploid DNA content.

Note: Supplementary data for this article are available at Cancer Research Online (<http://cancerres.aacrjournals.org/>).

Current address for M. Shago: Department of Paediatric Laboratory Medicine, The Hospital for Sick Children, 555 University Avenue, Toronto, Ontario, Canada M5G 1X8.

Requests for reprints: Linda Z. Penn, Division of Cancer Genomics and Proteomics, Ontario Cancer Institute, University of Toronto, 610 University Avenue, Room 9-628, Toronto, Ontario, Canada M5G 2M9. Phone: 416-946-2276; Fax: 416-946-2840; E-mail: lpenn@uhnres.utoronto.ca.

©2007 American Association for Cancer Research.

doi:10.1158/0008-5472.CAN-07-0644

Colony growth in soft agar. Anchorage-independent growth assays were conducted as described for Rat1a cells (7). The number of Rat1a colonies measuring >20 cells was assessed 3 weeks later. For SHEP Tet21/N-Myc cells, 10^4 cells were seeded in 10% FBS-RPMI 1640 + 0.3% noble agar in 35-mm Petri dishes and counted at the end of a 2-week period.

Coimmunoprecipitation. U2OS cells were exposed to 0.5 μ mol/L etoposide for 12 h and then harvested using immunoprecipitation lysis buffer (8). Extracts were immunoprecipitated with antibodies against CUL7 or p53 (DO-1). Immune complexes were collected with protein G-agarose beads and washed four times with wash buffer containing 5% sucrose, 5 mmol/L Tris-HCl (pH 7.4), 5 mmol/L EDTA, 0.5 mol/L NaCl, and 0.7% NP40.

CUL7 knockdown with RNAi. Oligos for CUL7 RNAi #2 were 5'-TGA-GATCTAGCTGAAGT-3' (forward) and 5'-CAGTTAAGCTAGGATCTCA-3' (reverse). Oligos for CUL7 RNAi #5 were 5'-AGAAGCTCCGCTACAGGGAATT-3' (forward) and 5'-AATTCCTGTAGCGGAGTTCT-3' (reverse). The control RNAi was against luciferase (9). Oligos were annealed and ligated into pLKO.1-puro, and together with pMD.G, pMDLg/pRRE and pRsv-Rev were transfected into 293TV cells to produce lentiviruses (10).

Purification of glutathione S-transferase-p53. Full-length p53 was cloned into GST2TK (Amersham) and purified as described previously (11).

In vitro translation and glutathione S-transferase pull-down assay. 35 S-labeled CUL7 proteins were prepared in reticulocyte lysate using the TNT system (Promega). Equal amounts of glutathione S-transferase (GST) and GST-p53 (10 μ g) immobilized on glutathione-Sepharose beads (GE) were incubated with labeled *in vitro* translated CUL7 proteins for 2 h at 4°C in the binding buffer [25 mmol/L Tris (pH 8.0), 150 mmol/L NaCl, 1 mmol/L EDTA, 1 mmol/L DTT, 10% glycerol, 0.2% NP40, 1 mmol/L phenylmethylsulfonyl fluoride]. The beads were washed extensively with the same buffer. The bound proteins were released with SDS sample buffer, separated by SDS-PAGE, and detected by autoradiography.

Generation of GST-p53 fusion proteins and use in CUL7(1-375) pull-down assays. Purified 1-70, 311-393, and 82-360 GST-fused p53 proteins were incubated with His-tagged CUL7(1-375) and then with the GST beads at 4°C for 1 h. After extensive washing with assay buffer, bound proteins were eluted with 20 mmol/L reduced glutathione and detected after SDS-PAGE by Coomassie Brilliant Blue.

Bioinformatics. The unprocessed data from microarray studies of tumor-normal differential expression in multiple sites, including lung (12, 13), prostate (14, 15), glioblastoma (16), and pancreas (14), were acquired. Following robust multichip analysis (RMA) preprocessing (17), we assessed differential CUL7 expression by comparing mean CUL7 mRNA levels in tumor samples with those in normal tissues separately for each study using a two-tailed *t* test with Welch's correction for unequal variances. Significant elevation ($P < 0.001$) of CUL7 mRNA was found in all studies of non-small cell lung cancers (12, 13). To determine if patient outcome is also related to CUL7 expression, we retrieved the unprocessed data for a large study of biomarkers in non-small cell lung cancer (18). Following RMA preprocessing (17), patients were median dichotomized according to CUL7 mRNA levels. The linear effect of CUL7 on survival was calculated using Cox proportional hazards modeling and the Wald test. All analysis was done in the R statistical environment (version 2.3.1) using the affy (version 1.10.0) and survival (version 2.29) packages.

Results and Discussion

Identification of an inhibitor of Myc-potentiated apoptosis.

To identify novel inhibitors of Myc-induced apoptosis, a functional screen was designed to identify cDNAs whose expression can block Myc-potentiated apoptosis (Fig. 1A). Rat1 cells expressing constitutive (*v-myc*) and inducible (*MycERtm*) *myc* allele, termed Rat1MycERtm-*myc* cells, were infected with a retroviral cDNA library (~2.7 million cDNAs) derived from a human breast carcinoma cell line, T47D. Two independent alleles of Myc were expressed in these cells to maximize apoptosis and reduce the outgrowth of false-positive clones. MycERtm was

activated with the addition of 4-hydroxytamoxifen to potentiate serum withdrawal-induced apoptosis, and the surviving cells were allowed to recover before being replated and subjected to a second round of selection. Cells that survived the second treatment were expanded and the cDNAs were recovered by PCR and tested for apoptosis-suppressing activity. From this screen, we identified and characterized three positive hits, including the well-established antiapoptotic Bcl2 and CUL7, a relatively new and unusually large member of the cullin family of proteins. Cullins, including CUL7, function as scaffold proteins to form either a Skp1-cullin-F-box (SCF) or SCF-like complex, which is involved in the process of protein ubiquitylation (8).

Understanding the biological role of CUL7 is in the earliest stages of exploration. CUL7 contributes to development, as knock-out mice are prenatal lethal (19), and germ-line mutations in humans result in 3M syndrome (20). A role for CUL7 as a positive regulator of cell proliferation has been proposed based on the slow growth phenotype of mouse embryonic fibroblasts (MEFs) derived from knockout mice (19) and the accelerated rate of cell proliferation following overexpression of CUL7 (21). However, a role for CUL7 as a negative regulator of cell proliferation has also been proposed based on the induction of apoptosis following CUL7 overexpression (22). Further, a SV40 large T antigen mutant incapable of binding CUL7 behaved similar to a p53-binding mutant and failed to promote anchorage-independent growth of MEFs (23). The reasons for these discrepancies remain unclear but may be a consequence of restricted, often single cell line analyses in either rodent or human systems (24).

Interestingly, results of our functional screen suggest a novel biological role for CUL7 in the etiology of cancer as an antiapoptotic oncogene that can cooperate with Myc in transformation. To further explore this hypothesis, it was important to first validate the screen and determine whether CUL7 can inhibit Myc-potentiated apoptosis in the cells used in the original screen. Rat1MycERtm-*myc* cells were infected with replication-incompetent control retrovirus and retrovirus carrying FLAG-CUL7 or Bcl2. The cells were then subjected to apoptosis induced by serum depletion and Myc activation, and the percentage of pre-G₁ cells (cell death) was determined by flow cytometry and propidium iodide staining. Like Bcl2, CUL7 was able to significantly inhibit Myc-potentiated apoptosis (Fig. 1B) when overexpressed (Fig. 1C).

CUL7 blocks both c-Myc-potentiated and N-Myc-potentiated apoptosis. To evaluate the functional role of CUL7 in independent cell systems, CUL7 or Bcl2 was first ectopically introduced into Rat1a cells expressing either control empty vector [green fluorescent protein (GFP) control] or ectopic c-Myc (Myc control; Fig. 2A and B). Rat1a cells are a transformed clone of Rat1 cells that are able to grow in an anchorage-independent manner when Myc is ectopically expressed in these cells (25). Rat1a cells expressing either control empty vector or ectopic c-Myc were subjected to serum withdrawal-induced apoptosis. As shown in Fig. 2A and B, cells expressing either ectopic CUL7 or Bcl2 were significantly more resistant to c-Myc-potentiated apoptosis compared with the Myc alone control (Myc control).

Next, we analyzed the effect of modulating CUL7 in human SHEP neuroblastoma cells, a tumor type with N-Myc deregulation central to etiology of disease. Knockdown of CUL7 expression using two independent siRNAs resulted in an increase in basal apoptosis compared with control cells (Fig. 2C, columns 2 and 3 compared with column 1). Together, these results indicate that CUL7 exerts antiapoptotic activity in cells that have been sentenced to die by either c-Myc or N-Myc.

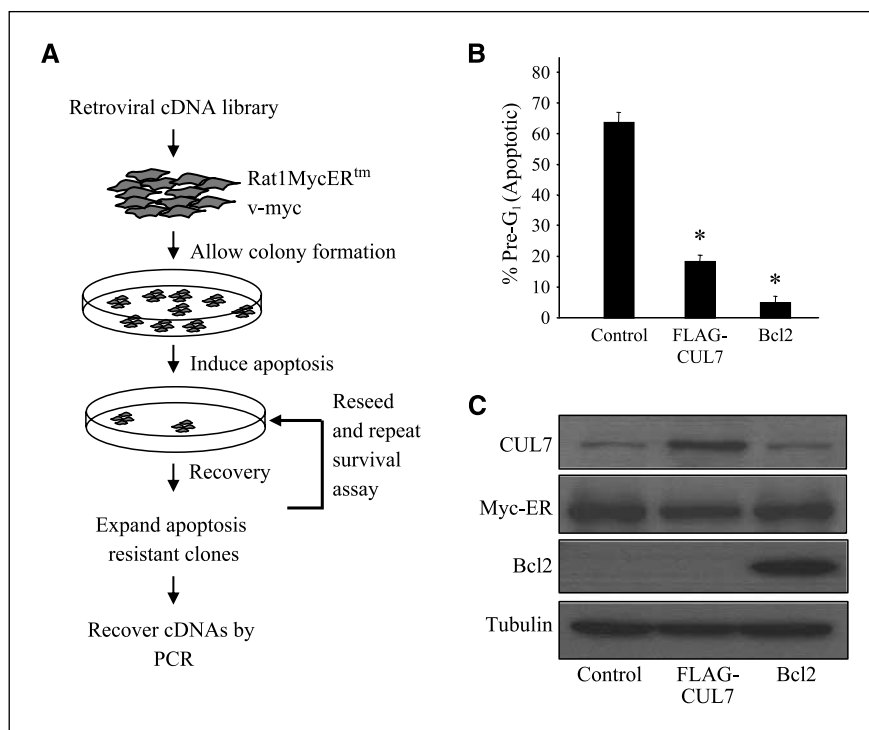


Figure 1. A functional screen identifies CUL7 as an inhibitor of Myc-induced apoptosis. *A*, schematic showing the functional screen used to identify expressed cDNAs whose products can block apoptosis induced by activation of Myc under low serum conditions. *B*, expression of FLAG-CUL7 or Bcl2 in Rat1MycERtm-v-myc cells blocks Myc-potentiated apoptosis in response to serum withdrawal as measured by flow cytometry and propidium iodide staining. Columns, mean of two separate experiments within which samples were measured in duplicate; bars, SD. *, difference when compared with the control empty vector is statistically significant ($P < 0.05$) using the pairwise *t* test. *C*, protein expression levels of CUL7, MycERtm, and Bcl2 in the Rat1MycERtm-v-myc cell lines ectopically expressing either control, FLAG-CUL7, or Bcl2 constructs.

Because Myc-induced apoptosis is broadly categorized as being p53 dependent or independent, we investigated which of these two pathways CUL7 targets. To determine whether p53 was essential for CUL7 to regulate apoptosis, we exogenously expressed control empty vector (MSCV-YFP) or a COOH-terminal fragment of p53 (MSCV-YFP-p53DD) into SHEP N-Myc neuroblastoma cells. Ectopic expression of p53DD, which encodes the COOH-terminal region (amino acids 302–390) of p53, binds to endogenous, wild-type, full-length p53 and significantly reduces p53 activity. To confirm that p53DD effectively functioned as a p53 dominant negative, we treated both SHEP YFP and SHEP p53DD YFP cells with doxorubicin for 24 h. As shown in Supplementary Fig. S1, expression of p53DD completely inhibited p53 from inducing one of its target genes, *PUMA*. SHEP YFP and SHEP p53DD YFP cells were then subsequently transduced with two independent CUL7 siRNAs to knock down endogenous CUL7 expression at the level of both protein (Fig. 2*D*, lanes 2, 3, 5, and 6) and mRNA (Supplementary Fig. S2*A*). Interestingly, p53 expression was consistently up-regulated in response to the knockdown of CUL7 (Fig. 2*D*, compare lanes 1–3). As mentioned above, SHEP N-Myc cells underwent significant cell death when CUL7 expression was knocked down (Fig. 2*C*, columns 1–3); however, when these cells expressed p53DD (Fig. 2*D*, lanes 4–6), the degree of apoptosis was decreased to basal levels (Fig. 2*C*, columns 4–6). Similar results were obtained when the experiment was repeated with terminal deoxynucleotidyl transferase-mediated dUTP nick end labeling staining as an alternative apoptosis assay (Supplementary Fig. S3). Furthermore, knockdown of CUL7 in ectopic Myc-expressing HCT116 cells (Supplementary Fig. S2*B*) promoted p53-dependent apoptosis triggered by 5-fluorouracil (Supplementary Fig. S4). Together, these data show that the antiapoptotic effect of CUL7 is p53 dependent.

CUL7 interacts with p53 both *in vivo* and *in vitro*. Because our data link CUL7 to p53-mediated apoptosis, we next investigated if CUL7 interacts with endogenous wild-type p53 *in vivo*.

The U2OS osteosarcoma cells are often used to study endogenous wild-type p53 because low basal p53 levels can be induced in response to etoposide. Thus, coimmunoprecipitation assays were conducted in etoposide-treated U2OS cells using either control preimmune serum or CUL7-specific antibody and immunoprecipitated proteins were then resolved by SDS-PAGE and immunoblotted using an anti-p53 (DO-1) antibody. Endogenous p53 was coimmunoprecipitated using the anti-CUL7 antibody (Fig. 3*A*, left), suggesting that endogenous CUL7 interacts with endogenous p53. The p53:CUL7 interaction was confirmed by reciprocal coimmunoprecipitation, which showed that CUL7 was coimmunoprecipitated using an anti-p53 antibody but not with an anti-GFP antibody (Fig. 3*A*, right).

To map the regions of CUL7 that interact with p53, GST pull-down assays were done using bacterially purified GST-tagged full-length p53 and ³⁵S-labeled CUL7 fragments synthesized by *in vitro* transcription and translation (Fig. 3*B*). Both NH₂-terminal and COOH-terminal regions of CUL7 show binding to p53 but not mid-region fragments (Fig. 3*B*). Our results extend a previous report that suggested that the p53:CUL7 interaction was restricted to the NH₂-terminal region of CUL7 (21, 26). This difference in results may be a consequence of our analyses being conducted *in vitro*, whereas that of the previous study was done *in vivo*. It is now appreciated that analysis *in vivo* may be confounded by alterations in subcellular localization of CUL7 mutants lacking the NH₂-terminal CPH (CUL7, PARC, HERC2) domain (amino acids 362–433; ref. 26). The CPH and COOH-terminal domain are thought to work in concert for p53:CUL7 to interact (27).

To determine whether the physical interaction between CUL7 and p53 is direct, a His-tagged CUL7 fragment (residues 1–375) and three GST-tagged p53 fragments (1–70, 82–360, and 311–393) were expressed in bacteria and purified. As shown in Fig. 3*C*, when His-CUL7(1–375) was coincubated with each GST-p53 fragment and subjected to GST pull-down assays, His-CUL7(1–375) strongly

bound both GST-p53(82-360) and GST-p53(311-393) but not GST-p53(1-70). These data show that CUL7 can bind to p53 directly in the absence of other proteins, such as the Skp1 or F-box proteins, which are required for SCF complex formation. Thus, CUL7 directly binds (Fig. 3C) and regulates p53 expression (Fig. 2D) by a mechanism that remains unclear (21).

CUL7 cooperates with Myc in transformation. Having shown that CUL7 is able to inhibit apoptosis induced by both c-Myc and N-Myc in a p53-dependent manner, we next tested the hypothesis that CUL7 functions as an oncogene and collaborates with Myc in transformation. Anchorage-independent growth was assessed in cells with and without ectopic expression of CUL7. Rat1a cells were first infected with control retrovirus or retrovirus containing c-Myc, and these two cell lines were then further infected with either control retrovirus or retroviruses containing FLAG-CUL7 or Bcl2. These Rat1a cells were then seeded in soft agar for 3 weeks

under either growth-promoting (10% serum) or apoptotic conditions (2% serum; ref. 7). Under growth-promoting conditions, the colony number was elevated in response to ectopic Myc expression as expected, and ectopic expression of CUL7 or Bcl2 in addition to ectopic expression of c-Myc did not result in increase in colony numbers (data not shown). By contrast, under apoptotic conditions, Rat1a cells coexpressing ectopic c-Myc with Bcl2 or CUL7 formed a significantly greater number of colonies compared with those cells expressing ectopic c-Myc alone (Fig. 4A). These data show that CUL7 cooperates with c-Myc to drive transformation specifically under apoptotic conditions, which is consistent with the antiapoptotic properties of CUL7 described here (Figs. 1B and 2A and C).

We next investigated if CUL7 similarly cooperates with N-Myc in allowing neuroblastoma cells to grow in an anchorage-independent manner. We used SHEP cells, where N-Myc expression can be controlled using tetracycline, and introduced either control siRNA or

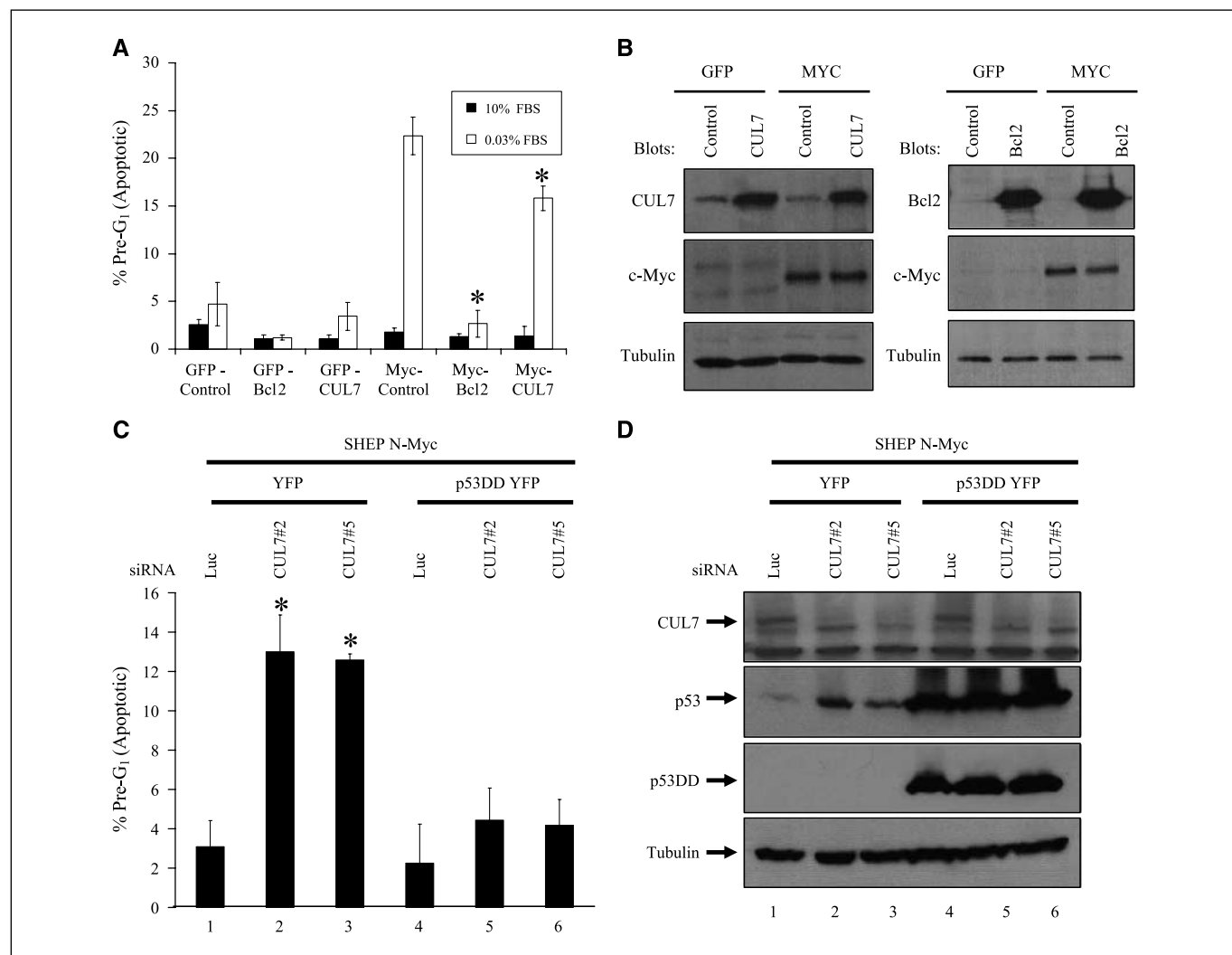


Figure 2. CUL7 inhibits Myc-potentiated apoptosis and cooperates with Myc in transformation. *A*, expression of FLAG-CUL7 or Bcl2 in Rat1a cells blocks Myc-potentiated apoptosis in response to serum withdrawal as measured by flow cytometry combined with propidium iodide staining. *Columns*, mean of two separate experiments where each experiment was composed of measurements of triplicate samples per experimental group; *bars*, SD. *, difference when compared with the control empty vector is statistically significant ($P < 0.05$) using the pairwise *t* test. *B*, protein expression levels of CUL7, Myc, and Bcl2 in the Rat1a cell line. *C*, CUL7 inactivation by siRNA triggers SHEP N-Myc neuroblastoma cells to undergo p53-dependent cell death. *Columns*, percentage of cells showing a pre-G₁ DNA content expressed as the mean of three independent experiments, where each experiment was composed of measurements of triplicate samples per experimental group; *bars*, SD. *, statistically significant difference compared with the SHEP MSCV-YFP control luciferase siRNA cells ($P < 0.05$) using the pairwise *t* test. *D*, endogenous CUL7 was knocked down by siRNA in SHEP N-Myc cells overexpressing either control MSCV-YFP or MSCV-YFP-p53DD, and immunoblot analysis was done.

two independent CUL7 siRNAs into these cells. These cells were then seeded in a soft agar and colonies were counted after 2 weeks. As shown in Fig. 4B and Supplementary Fig. S5, SHEP cells expressing ectopic N-Myc and endogenous levels of CUL7 grew robustly in an anchorage-independent manner to form colonies. However, the cells where N-Myc was turned off, or where CUL7 expression had been knocked down, formed significantly fewer colonies. Similar results were also observed when CUL7 expression was knocked down in MCF7 cells (data not shown). These data suggest that high expression of both Myc and CUL7 is required for the anchorage-independent growth of tumor cells and that these two genes are cooperating to promote transformation.

As a negative regulator of apoptosis, CUL7 may be deregulated in human cancers. To test this hypothesis, we used *in silico* analysis of multiple public microarray studies (12–16). Interestingly, CUL7 mRNA was significantly elevated relative to normal in two studies (12, 13) of non-small cell lung cancer but not in prostate (14, 15), glioblastoma (16), and pancreas (Fig. 4C; ref. 14). This suggests that overexpression of CUL7 mRNA confers a survival advantage to tumors in a tissue-specific manner. Indeed, our data are consistent with the finding that the most profound effect of CUL7 knockout

was on lung development and that this resulted in postnatal death (19). Because CUL7 is significantly overexpressed in lung tumors compared with normal lung, this raised the possibility that CUL7 expression is also associated with disease progression. To evaluate this possibility, we used a recent microarray study of prognostic markers in non-small cell lung cancers (18). We split the patient population into two groups based on their CUL7 expression levels and found that patients with elevated CUL7 mRNA levels showed significantly ($P = 0.02$) reduced survival (Fig. 4D). Specifically, a 2-fold increase in CUL7 expression confers a 2.8-fold increase in hazard for the patient. Similar results were observed with both alternative CUL7 ProbeSets and a second array data set (12). These primary tumor data (Fig. 4C and D) provide strong evidence that CUL7 expression is deregulated in primary lung cancers and that this deregulation is associated with poor patient outcome.

Over the last 5 years since CUL7 was first described (8), it has been shown that CUL7 can function as a regulator of cell proliferation. CUL7 knockout MEFs displayed a slow growth phenotype (19), overexpression of CUL7 accelerated cell proliferation in a p53-dependent manner (21), and the knockdown of CUL7 induced p53-dependent growth arrest (28). Moreover, 3M syndrome, a

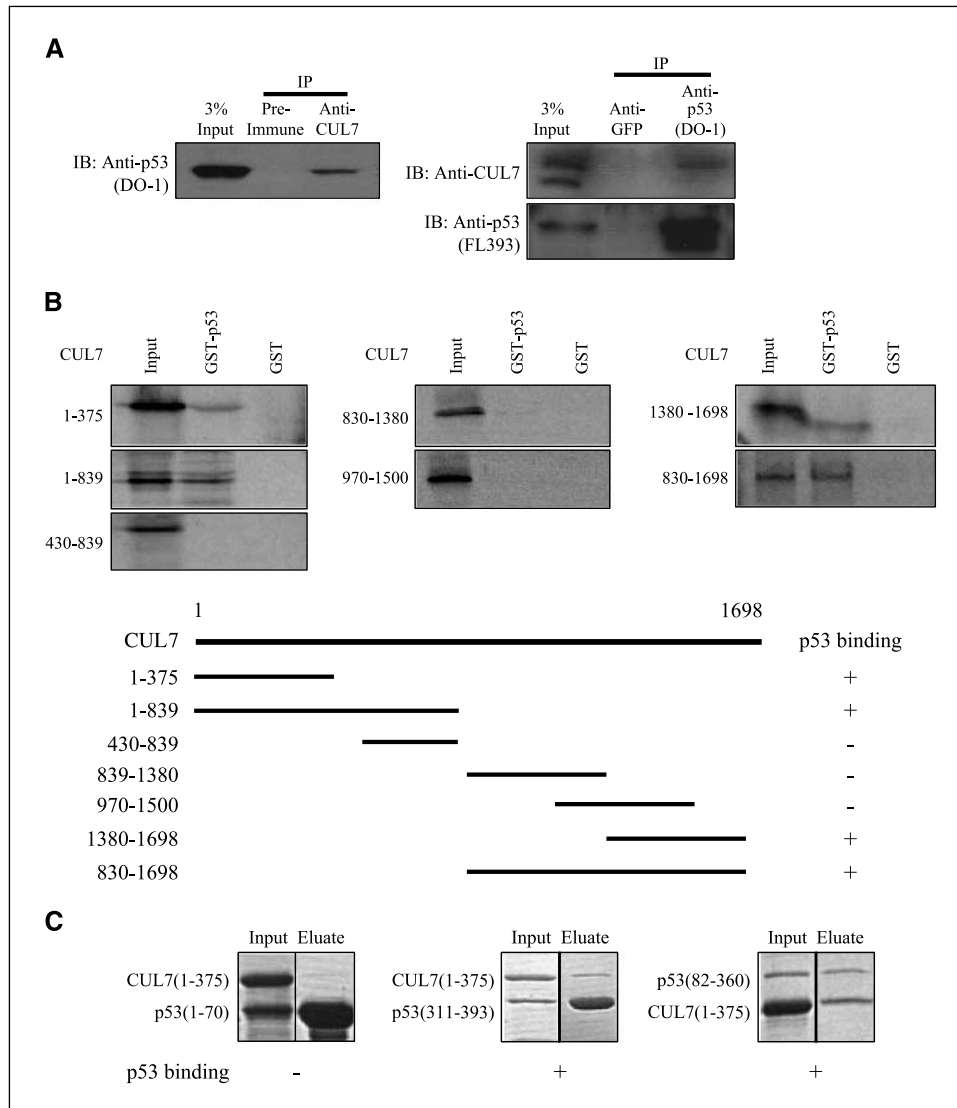
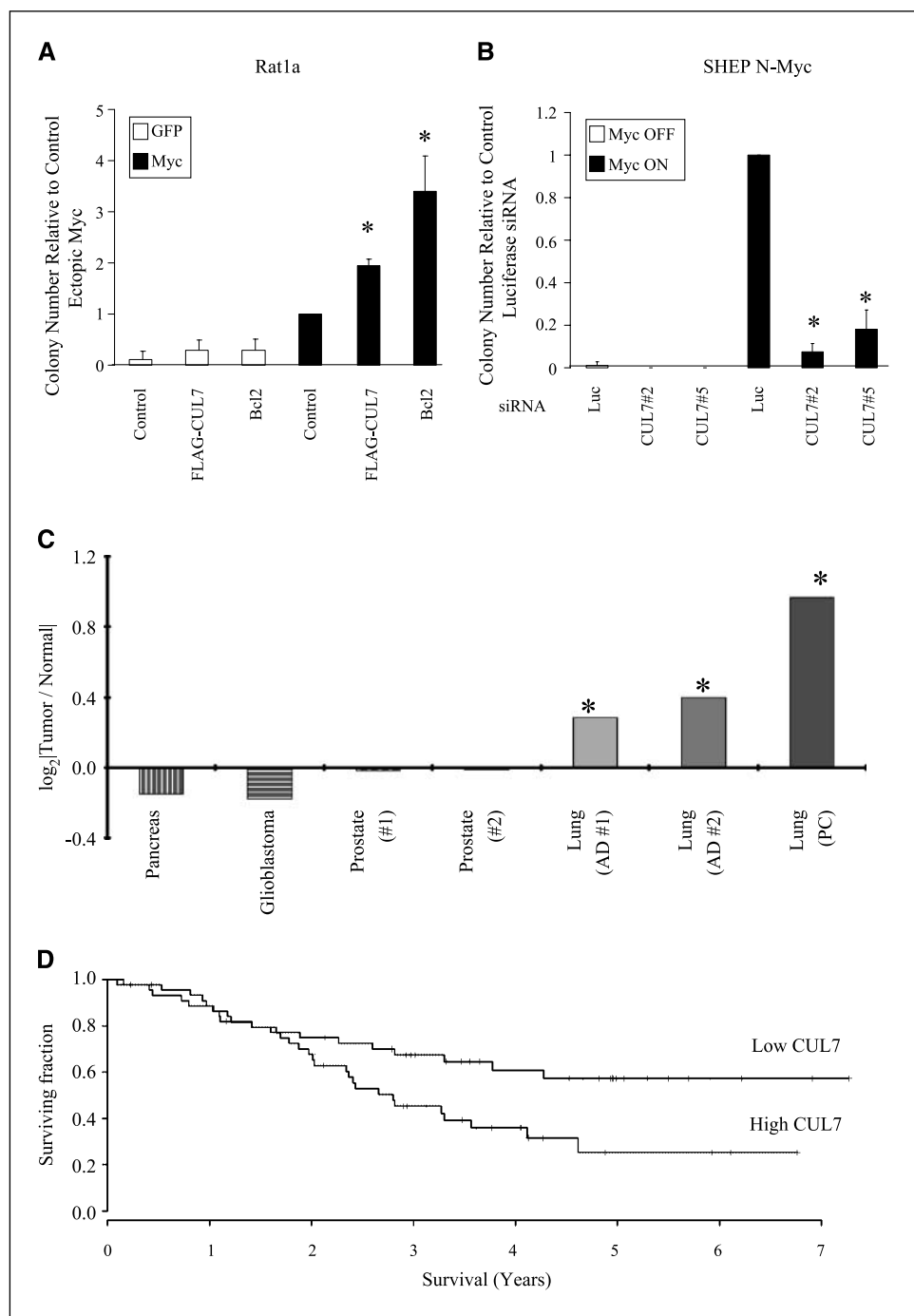


Figure 3. CUL7 and p53 interact *in vivo* and *in vitro*. **A, left**, U2OS cells were exposed to 0.5 $\mu\text{mol/L}$ etoposide for 12 h to induce endogenous p53 and then harvested. Proteins were immunoprecipitated (IP) using the preimmune serum or a CUL7-specific antibody and then immunoblotted (IB) with anti-p53 antibody (DO-1). **Right**, reciprocal immunoprecipitation was carried out using anti-GFP antibody (control) or anti-p53 (DO-1) antibody to immunoprecipitated proteins followed by immunoblotting with anti-CUL7 and anti-p53 antibody (FL393). **B**, both the N terminus and C terminus of CUL7, but not the central region, interact with GST-p53. The *in vitro* transcribed and translated ^{35}S -labeled CUL7 fragments (Input) were incubated with GST-p53 and GST, and GST pull-down experiments were conducted. Bound proteins were separated by SDS-PAGE and detected by autoradiography. Schematic representation of the deletion mutants of CUL7 and its p53 binding. **C**, CUL7 interacts with p53 directly *in vitro*. Bacterially expressed and purified GST-p53 fragments were coincubated with the His-CUL7(1-375) polypeptide (Input) and mixed with glutathione-Sepharose beads. After washing, proteins were eluted with glutathione (Eluate). Binding was observed between CUL7(1-375) with p53 fragments 82-360 and 311-393 but not p53(1-70).

Figure 4. CUL7 collaborates with Myc in transformation and is overexpressed and associated with poor prognosis in lung cancer. **A**, CUL7 cooperates with c-Myc to potentiate Rat1a colony growth in soft agar under low serum conditions. *Columns*, colony numbers relative to Rat1a-Myc with control empty vector expressed as the mean of three separate experiments, where each experiment was composed of measurements of triplicate samples per experimental group; *bars*, SD. *, statistically significant difference compared with the control empty vector ($P < 0.05$) using the pairwise *t* test. **B**, down-regulation of N-Myc or CUL7 in SHEP N-Myc neuroblastoma cells results in significant loss of anchorage-independent growth. *Columns*, colony numbers relative to control siRNA expressed as the mean of two separate experiments, where each experiment was composed of measurements of triplicate samples per experimental group; *bars*, SD. *, statistically significant difference compared with the control luciferase siRNA ($P < 0.05$) using the paired *t* test. **C**, to determine if CUL7 plays a role in primary human cancer, we compared the levels of CUL7 mRNA in normal and tumor tissues in public microarray studies. For each study, the ratio of mean expression levels between tumor and normal tissues was calculated and \log_2 transformed. Differential expression was assessed using a two-tailed *t* test with Welch's correction, and the \log_2 ratio values are plotted separately for each study. References to each study are given in the text. For lung tumors, two histologic types were considered: adenocarcinomas (AD) and pulmonary carcinoids (PC). *, statistically significant difference in mean expression levels between tumor and normal ($P < 0.001$). **D**, elevated expression of CUL7 mRNA is associated with poor prognosis. Patient samples in a microarray study of non-small cell lung cancers were median dichotomized according to CUL7 mRNA levels and patient survival differences were plotted. Cox proportional hazards analysis shows that patients with higher CUL7 expression have significantly lower survival (hazard ratio, 2.83; 95% confidence interval, 1.04–7.70; $P = 0.04$).



human disease caused by intrauterine growth retardation, is linked to various CUL7 mutations (20).

Our study clearly indicates that CUL7 is an oncogene that can play a role in the etiology of human cancer. Unlike the role of CUL7 in cell growth, the role of CUL7 in apoptosis has remained largely unaddressed. Although it has been reported that expression of mouse CUL7 triggers apoptosis when ectopically expressed in NIH 3T3 cells (22), we have shown that ectopic expression of human CUL7 in rat cells protected them from Myc-potentiated apoptosis. We have also shown that knockdown of human CUL7 triggered p53-dependent apoptosis in several cell lines derived from a variety of human cancers, including neuroblastoma and colon. Interest-

ingly, the role of CUL7 in the control of cell growth and death seems functionally linked to p53 (24).

The mechanism by which CUL7 regulates p53 remains unclear; however, two working models under consideration propose that CUL7 controls p53 ubiquitylation and/or subcellular localization. CUL7 can function as an E3 ubiquitin ligase (8, 20), suggesting that CUL7 may negatively regulate p53 by ubiquitylating and targeting it for degradation. This model is consistent with a recent report indicating that DNA damage can induce CUL7 expression leading to a decrease in p53 expression (28). However, two independent groups showed that overexpression of CUL7 and p53 *in vivo* did not result in an increase of ubiquitylated p53

(21, 28). By contrast, *in vitro* ubiquitylation experiments by Andrews et al. (21) showed that CUL7 can monoubiquitylate or diubiquitylate p53. The second mechanistic model under consideration is based on the amino acid similarity of CUL7 with PARC, a protein reported to inhibit p53 activity by anchoring it in the cytoplasm (29). In particular, these proteins are founding members of the new CPH structural domain shown to be important for direct interaction with p53 (Fig. 3; ref. 27). However, Andrews et al. showed that coexpression of CUL7 together with p53 did not significantly alter p53 localization, suggesting that CUL7 does not inhibit p53 activity in a similar manner as PARC. Taken together, it is not yet clear how CUL7 regulates the p53 tumor suppressor.

In this article, we not only show that CUL7 can bind directly to p53 and protect cells from p53-dependent apoptosis but that CUL7 can cooperate with both c-Myc and N-Myc to promote anchorage-independent growth in multiple cell systems. This is an interesting finding as it suggests that CUL7 may play an important role in the transformation of normal cells to tumor cells. Indeed, we show that CUL7 is also overexpressed in human lung cancers and that increased expression is correlated with poor patient outcome. Other proteins deregulated in lung cancer, such as EGFR,

have been specifically targeted pharmacologically (i.e., gefitinib), resulting in improved clinical outcome (30). Because our data indicate that CUL7 is also highly deregulated in lung tumors and associated with poor patient outcome, pharmacologic inhibition of CUL7 may be a valuable strategy for treating lung cancers, as well as other human cancers, with deregulated CUL7 expression.

Acknowledgments

Received 2/15/2007; revised 7/4/2007; accepted 8/31/2007.

Grant support: Canadian Institutes of Health Research operating grants (L.Z. Penn), and Canada Research Chairs Program (CHA), Canadian Cancer Society operating grant (C. Arrowsmith), Natural Science and Engineering Research Council Awards (S.S. Kim, P.C. Boutros, D.Y.L. Mao, and J.W. Clendening), Canadian Institutes of Health Research fellowship (G.A. Trentin and D. Barsyte-Lovejoy), Excellence in Radiation Research for the 21st Century Strategic Training Initiative in Health Research program funded by the Canadian Institutes of Health Research (P.C. Boutros and J.W. Clendening), Precarn fellowship (P.C. Boutros), Leukemia and Lymphoma Society of Canada fellowship (L. Kaustov and Y. Sheng), and National Cancer Institute of Canada fellowship (Y. Sheng).

The costs of publication of this article were defrayed in part by the payment of page charges. This article must therefore be hereby marked *advertisement* in accordance with 18 U.S.C. Section 1734 solely to indicate this fact.

We thank Dr. Moshe Oren for the p53DD plasmid, M. Schwab and S. Hann for providing us with SHEP Tet21/N-Myc and Rat1a cell lines, Dr. David Andrews for anti-Bcl2 antibody, and our colleagues in the Penn laboratory for helpful discussions.

References

- Oster SK, Ho CS, Soucie EL, Penn LZ. The myc oncogene: Marvelously Complex. *Adv Cancer Res* 2002; 84:81–154.
- Evan GI, Wyllie AH, Gilbert CS, et al. Induction of apoptosis in fibroblasts by c-myc protein. *Cell* 1992;69: 119–28.
- Lindstrom MS, Klangby U, Wiman KG. p14ARF homozygous deletion or MDM2 overexpression in Burkitt lymphoma lines carrying wild type p53. *Oncogene* 2001; 20:2171–7.
- Brodeur GM. Neuroblastoma: biological insights into a clinical enigma. *Nat Rev Cancer* 2003;3:203–16.
- Oster SK, Marhin WW, Asker C, et al. Myc is an essential negative regulator of platelet-derived growth factor β receptor expression. *Mol Cell Biol* 2000;20:6768–78.
- Whitehead I, Kirk H, Kay R. Expression cloning of oncogenes by retroviral transfer of cDNA libraries. *Mol Cell Biol* 1995;15:704–10.
- Conzen SD, Gottlob K, Kandel ES, et al. Induction of cell cycle progression and acceleration of apoptosis are two separable functions of c-Myc: transrepression correlates with acceleration of apoptosis. *Mol Cell Biol* 2000;20:6008–18.
- Dias DC, Dolios G, Wang R, Pan ZQ. CUL7: A DOC domain-containing cullin selectively binds Skp1.Fbx29 to form an SCF-like complex. *Proc Natl Acad Sci U S A* 2002;99:16601–6.
- Paddison PJ, Caudy AA, Bernstein E, Hannon GJ, Conklin DS. Short hairpin RNAs (shRNAs) induce sequence-specific silencing in mammalian cells. *Genes Dev* 2002;16:948–58.
- Barsyte-Lovejoy D, Lau SK, Boutros PC, et al. The c-Myc oncogene directly induces the H19 noncoding RNA by allele-specific binding to potentiate tumorigenesis. *Cancer Res* 2006;66:5330–7.
- Ruppert JM, Stillman B. Analysis of a protein-binding domain of p53. *Mol Cell Biol* 1993;13:3811–20.
- Beer DG, Kardias SL, Huang CC, et al. Gene-expression profiles predict survival of patients with lung adenocarcinoma. *Nat Med* 2002;8:816–24.
- Bhattacharjee A, Richards WG, Staunton J, et al. Classification of human lung carcinomas by mRNA expression profiling reveals distinct adenocarcinoma subclasses. *Proc Natl Acad Sci U S A* 2001;98:13790–5.
- Ramaswamy S, Tamayo P, Rifkin R, et al. Multiclass cancer diagnosis using tumor gene expression signatures. *Proc Natl Acad Sci U S A* 2001;98:15149–54.
- Singh D, Febbo PG, Ross K, et al. Gene expression correlates of clinical prostate cancer behavior. *Cancer Cell* 2002;1:203–9.
- Nigro JM, Misra A, Zhang L, et al. Integrated array-comparative genomic hybridization and expression array profiles identify clinically relevant molecular subtypes of glioblastoma. *Cancer Res* 2005;65:1678–86.
- Irizarry RA, Bolstad BM, Collin F, Cope LM, Hobbs B, Speed TP. Summaries of Affymetrix GeneChip probe level data. *Nucleic Acids Res* 2003;31:e15.
- Bild AH, Yao G, Chang JT, et al. Oncogenic pathway signatures in human cancers as a guide to targeted therapies. *Nature* 2006;439:353–7.
- Arai T, Kasper JS, Skaar JR, Ali SH, Takahashi C, DeCaprio JA. Targeted disruption of p185/Cul7 gene results in abnormal vascular morphogenesis. *Proc Natl Acad Sci U S A* 2003;100:9855–60.
- Huber C, Dias-Santagata D, Glaser A, et al. Identification of mutations in CUL7 in 3-M syndrome. *Nat Genet* 2005;37:1119–24.
- Andrews P, He YJ, Xiong Y. Cytoplasmic localized ubiquitin ligase cullin 7 binds to p53 and promotes cell growth by antagonizing p53 function. *Oncogene* 2006;25:4534–48.
- Tsai SC, Pasumarthi KB, Pajak L, et al. Simian virus 40 large T antigen binds a novel Bcl-2 homology domain 3-containing proapoptosis protein in the cytoplasm. *J Biol Chem* 2000;275:3239–46.
- Ali SH, Kasper JS, Arai T, DeCaprio JA. Cul7/p185/p193 binding to simian virus 40 large T antigen has a role in cellular transformation. *J Virol* 2004;78:2749–57.
- Dowell JD, Tsai SC, Dias-Santagata DC, et al. Expression of a mutant p193/CUL7 molecule confers resistance to MG132- and etoposide-induced apoptosis independent of p53 or Parc binding. *Biochim Biophys Acta* 2007;1773:358–66.
- Stone J, de Lange T, Ramsay G, et al. Definition of regions in human c-myc that are involved in transformation and nuclear localization. *Mol Cell Biol* 1987;7:1697–709.
- Kasper JS, Arai T, DeCaprio JA. A novel p53-binding domain in CUL7. *Biochem Biophys Res Commun* 2006; 348:132–8.
- Kaustov L, Lukin J, Lemak A, et al. The conserved CPH domains of Cul7 and PARC are protein-protein interaction modules that bind the tetramerization domain of p53. *J Biol Chem* 2007;282:11300–7.
- Jung P, Verdoodt B, Bailey A, Yates JR III, Menssen A, Hermeking H. Induction of Cullin 7 by DNA damage attenuates p53 function. *Proc Natl Acad Sci U S A* 2007; 104:11388–93.
- Nikolaev AY, Li M, Puskas N, Qin J, Gu W. Parc: a cytoplasmic anchor for p53. *Cell* 2003;112:29–40.
- Paez JG, Janne PA, Lee JC, et al. EGFR mutations in lung cancer: correlation with clinical response to gefitinib therapy. *Science* 2004;304:1497–500.